CDDpress

www.nature.com/cddiscovery

ARTICLE OPEN

Overexpressing eukaryotic elongation factor 1 alpha (eEF1A) proteins to promote corticospinal axon repair after injury

Daniel Romaus-Sanjurjo[1,4], Junmi M. Saikia[1,2], Hugo J. Kim[1], Kristen M. Tsai[1], Geneva Q. Le[1] and Binhai Zheng[1,3]✉

Although protein synthesis is hypothesized to have a pivotal role in axonal repair after central nervous system (CNS) injury, the role of core components of the protein synthesis machinery has not been examined. Notably, some elongation factors possess non-canonical functions that may further impact axonal repair. Here, we examined whether overexpressing eukaryotic elongation factor 1 alpha (eEF1A) proteins enhances the collateral sprouting of corticospinal tract (CST) neurons after unilateral pyramidotomy, along with the underlying molecular mechanisms. We found that overexpressing eEF1A proteins in CST neurons increased the levels of pS6, an indicator for mTOR activity, but not pSTAT3 and pAKT levels, in neuronal somas. Strikingly, overexpressing eEF1A2 alone, but neither eEF1A1 alone nor both factors simultaneously, increased protein synthesis and actin rearrangement in CST neurons. While eEF1A1 overexpression only slightly enhanced CST sprouting after pyramidotomy, eEF1A2 overexpression substantially enhanced this sprouting. Surprisingly, co-overexpression of both eEF1A1 and eEF1A2 led to a sprouting phenotype similar to wild-type controls, suggesting an antagonistic effect of overexpressing both proteins. These data provide the first evidence that overexpressing a core component of the translation machinery, eEF1A2, enhances CST sprouting, likely by a combination of increased protein synthesis, mTOR signaling and actin cytoskeleton rearrangement.

Cell Death Discovery (2022)8:390 ; https://doi.org/10.1038/s41420-022-01186-z

INTRODUCTION

Spinal cord injury often causes an irreversible loss of function which is due in part to the damage of the corticospinal tract (CST). Since the CST contributes significantly to the control of skilled motor movements in humans, unraveling the mechanisms of axonal repair for the CST will benefit therapeutic development for spinal cord injury. Compared with the regeneration of injured axons, compensatory sprouting of uninjured axons represents a more accessible form of axonal repair for clinical translation due to three factors: the existence of spared axonal pathways in the majority of spinal cord injury patients, a higher level of intrinsic axon growth ability of uninjured neurons, and a lower barrier to attain and enhance sprouting [1].

mRNA translation is a key process in cellular metabolism that leads to protein synthesis. During translation elongation, eEF1A proteins carry out the critical step of recruiting aminoacyl-tRNAs to the A site of the ribosome [2, 3]. There are two eEF1A proteins, eEF1A1 and eEF1A2, encoded by two different genes with different expression patterns: eEF1A1 is present in all adult tissues but muscle, heart, and neurons (except for some small neurons); while eEF1A2 is highly expressed in muscle and heart tissues as well as neurons [4–6]. Following axonal damage, the capacity of neurons to synthesize new proteins is crucial for their regenerative ability [7]. Indeed, the mTOR pathway is a key regulator of CNS axon regeneration [8, 9], partially by activating protein synthesis via the eukaryotic initiation factor 4E (eIF4E) [10, 11]. Recently, manipulating eEF1A2 was found to enhance protein translation in vitro in a study of dendritic spine remodeling [12]. Given that both eEF1A1 and eEF1A2 carry out a pivotal function during protein synthesis, they are interesting targets to increase the rate of protein synthesis underlying axon growth.

In addition to their role in protein synthesis, eEF1A proteins also have non-canonical roles. They can promote cell growth and proliferation by serving as upstream activators of PI3K/AKT/mTOR or PI3K/AKT/STAT3 pathways [13–15]. Moreover, eEF1A proteins possess actin-binding domains that enable a role in actin-bundling and cytoskeleton organization in vivo [16–20]. Along these lines, the most recent data have revealed that eEF1A2 deficient neurons exhibit shorter neurite length [21]. This is relevant following axonal damage since actin dynamics have a key role in the formation of a competent growth cone, which is vital for proper axon growth and regeneration [22–24]. Overall, the literature has implicated a role for eEF1A proteins in cellular processes deemed important for axonal repair.

These considerations prompted us to test the possibility that manipulating eEF1A proteins through virally mediated overexpression could enhance compensatory CST sprouting after a unilateral pyramidotomy injury by boosting protein translation and cytoskeleton rearrangement as well as activating downstream neuron-intrinsic pathways. Our data provide the first in vivo demonstration to our knowledge that manipulating a core component of the translational machinery can enhance axonal repair in the mammalian CNS.

[1]Department of Neurosciences, School of Medicine, University of California San Diego, La Jolla, CA 92093, USA. [2]Neurosciences Graduate Program, University of California San Diego, La Jolla, CA 92093, USA. [3]VA San Diego Research Service, San Diego, CA 92161, USA. [4]Present address: NeuroAging Group (NEURAL), Clinical Neurosciences Research Laboratories (LINCs), Health Research Institute of Santiago de Compostela (IDIS), 15706 Santiago de Compostela, Spain. ✉email: bizheng@health.ucsd.edu

Received: 9 June 2022 Revised: 1 September 2022 Accepted: 7 September 2022
Published online: 20 September 2022

RESULTS

Cortical injections of AAV-eEF1A1 or AAV-eEF1A2 increase the expression of eEF1A1 and eEF1A2 proteins respectively in CST neurons

Prior to testing our hypothesis, we first validated the effect of injecting AAV-eEF1A1 or AAV-eEF1A2 in CST neurons of layer V cortex. These CST neurons are identifiable based on their larger size compared to other counterparts, positive staining for NeuN and GFP, and anatomical location in cortical layer V. In eEF1A1 OE mice, eEF1A1 immunoreactivity in GFP^+ CST neurons was increased by 29.2% as compared with control mice (Mann–Whitney U, $p < 0.0001$; Fig. 1A–B‴, F). Following eEF1A2 overexpression, GFP^+ CST neurons showed a significant 38.5% increase in the eEF1A2 immunoreactivity compared with controls (Mann–Whitney U, $p < 0.0001$; Fig. 1C–D‴, G). In agreement with previous work [6], the expression of eEF1A1 in controls is lower than eEF1A2 (Fig. 1B, D). In eEF1A1 and eEF1A2 co-overexpressing (eEF1As OE) mice, overexpression levels of each eEF1A protein were similar to those from eEF1A1 and eEF1A2 single OE mice (Fig. 1H, S1C). Consistent with the GFP-fusion expression constructs, the GFP signals from AAV-eEF1A1::GFP and AAV-eEF1A2::GFP co-labeled with elevated eEF1A1 and eEF1A2 signals, respectively (Fig. 1A″, C″, S1C). These data confirmed that each viral vector led to the overexpression of the respective eEF1A protein in CST neurons.

Overexpressing eEF1A2 significantly increases protein synthesis in CST neurons

Given that eEF1A proteins play a pivotal role during mRNA translation [2, 12], we examined the effect of overexpressing either eEF1A1 or eEF1A2 on protein synthesis in CST neurons (Fig. 2). We used a puromycin-based assay, Surface Sensing of Translation (SUnSET), previously adapted for use in vivo [25, 26]. The SUnSET assay showed that eEF1A1 overexpression exhibited a trend for increased protein synthesis in CST neurons that did not reach statistical significance (Fig. 2B–B‴, F). In contrast, overexpressing eEF1A2 significantly albeit modestly increased protein synthesis (by ~9%) compared to control (Kruskal–Wallis, $p = 0.0239$; Fig. 2C–C‴, F). Unexpectedly, co-overexpressing both eEF1A1 and eEF1A2 simultaneously did not further increase protein synthesis, and if anything, may have slightly reduced protein synthesis (Fig. 2D–D‴, F). We used PTEN cKO mice as a positive control since PTEN deletion is known to enhance CST regeneration and the mTOR pathway regulates global translation [10]. Unsurprisingly, these mice exhibited a more substantial ~30% increase in protein translation (Kruskal–Wallis, $p = 0.0011$; Fig. 2E–E″, F). Together, these results revealed that only the overexpression of eEF1A2 led to a significant increase in mRNA translation.

Overexpressing eEF1A1 and eEF1A2 impacts mTOR and STAT3 pathways differently in CST neurons

eEF1A proteins can act as upstream activators of mTOR and STAT3 pathways in non-neuronal cells [13, 14], both of which are known regulators of CST axon sprouting after CNS injury [8, 27]. Immunohistochemistry revealed an increase in the levels of pS6, a marker for mTOR activity, following eEF1A1 OE (33.9%), eEF1A2 OE (37%) or co-overexpression (33.1%) in CST neurons compared to controls (Kruskal–Wallis, $p < 0.0001$ for all; Fig. 3). As a positive control, PTEN deletion increased pS6 levels by a large 106% as compared to controls (Kruskal–Wallis, $p < 0.0001$; Fig. 3E–E″, F). In contrast, no significant differences were found in pSTAT3 immunostaining among mice overexpressing eEF1A1, eEF1A2, both proteins, and control mice (Kruskal–Wallis; Fig. 4). Together, these results indicate that overexpressing eEF1A proteins alone or in combination moderately activated the mTOR pathway as previously seen in non-neuronal cells, but had no detectable effect on the STAT3 pathway.

Overexpressing eEF1A2 but not eEF1A1 promotes actin rearrangement

eEF1A proteins possess actin-binding domains that enable a role in actin-bundling and cytoskeleton organization in vivo and in vitro [16, 17]. Thus, we examined the impact of overexpressing eEF1A proteins on actin remodeling. Whereas control, eEF1A1 OE and eEF1As OE mice displayed a diffuse pattern of beta Actin expression (Fig. 5A, S3); this pattern appeared bundled in eEF1A2 OE mice, defining the cellular shape (Fig. 5B, S3, arrowheads). This qualitative observation was corroborated with immunohistochemical quantifications, which revealed a significant increase of actin signal intensity only in eEF1A2 OE mice (one-way ANOVA, $p = 0.0054$ vs Control, $p = 0.0018$ vs eEF1A1; Fig. 5C). Co-overexpressing both eEF1A1 and eEF1A2 simultaneously decreased the actin signal compared to eEF1A2 OE mice ($p = 0.0586$; Fig. 5C). Interestingly, a few $GFP^-/GFAP^+$ astrocytes (Fig. 5, thick arrows) and many $GFP^-/GFAP^-/NeuN^-$ cells (Fig. 5, thin arrows) from eEF1A2 OE mice also showed bundled beta actin expression. Overall, this raises the possibility that the over-expression of eEF1A2 alters actin dynamics by bundling actin not only directly in neurons but also indirectly in non-neuronal cells through an unknown neuron-glia crosstalk mechanism.

Neither eEF1A1 overexpression nor eEF1A2 overexpression increases the level of pAKT in CST neurons

Given that AKT is involved in both the activation of the mTOR signaling [28] and actin remodeling [16], we examined the levels of AKT activation following eEF1A and PTEN manipulations. Neither eEF1A1 nor eEF1A2 overexpression increased the level of AKT phosphorylation (pAKT); PTEN deletion exhibited a trend for increased pAKT levels that did not reach statistical significance (Kruskal–Wallis; Fig. 6). Therefore, we cannot resolve whether eEF1A-mediated mTOR activation or eEF1A2-mediated actin rearrangement goes through AKT signaling.

Overexpressing eEF1A2 promotes CST sprouting more than eEF1A1

After undergoing unilateral pyramidotomy (Fig. 7A–D, I–J), eEF1A1 OE mice only exhibited a significant increase in the number of axons just crossing the midline at 50 µm compared to GFP control mice (two-way repeated measures [RM] ANOVA with Tukey post hoc test, $p = 0.0106$) (Fig. 7B, I). In contrast, eEF1A2 OE mice exhibited significantly elevated levels of CST sprouting up to 200 µm past the midline (two-way RM ANOVA with Tukey's correction; $p = 0.0006$ at 50 µm; $p = 0.0101$ at 100 µm; and $p = 0.0044$ at 200 µm) (Fig. 7C, I). Interestingly, the sprouting indices from eEF1A2 OE mice approached those from PTEN cKO mice, where the two groups did not exhibit statistically significant differences (two-way RM ANOVA with Tukey's correction) (Fig. S2). Co-overexpressing both eEF1A1 and eEF1A2 unexpectedly suppressed this enhancement in CST sprouting (Fig. 7A, D, I) such that the level of CST sprouting in eEF1A2 OE mice was significantly higher than that in eEF1As mice at 200 µm (two-way RM ANOVA with Tukey's correction; $p = 0.0403$; Fig. 7I).

Intriguingly, control mice with AAV-GFP injections exhibited GFP signals in the medulla, where mice injected with the AAV-eEF1A1::GFP or AAV-eEF1A2::GFP fusion construct had no detectable GFP signals (Fig. 7E–H). As a comparison, all mice exhibited robust BDA signals at the medulla level (Fig. 7E–H). This result suggests that the fusion proteins did not reach the axons at detectable levels. Thus, any overexpressed eEF1A protein likely acted in the somas and not axons (or dendrites) to enhance CST axon sprouting as might have been expected from the literature [12, 29, 30]. Together, these data suggest that overexpressing eEF1A1 and even more so eEF1A2 enhances CST sprouting through a mechanism in the neuronal somas.

DISCUSSION

In this study, we have provided gain-of-function data showing that virally mediated overexpression of eEF1A proteins and especially eEF1A2 enhances axon sprouting of CST neurons

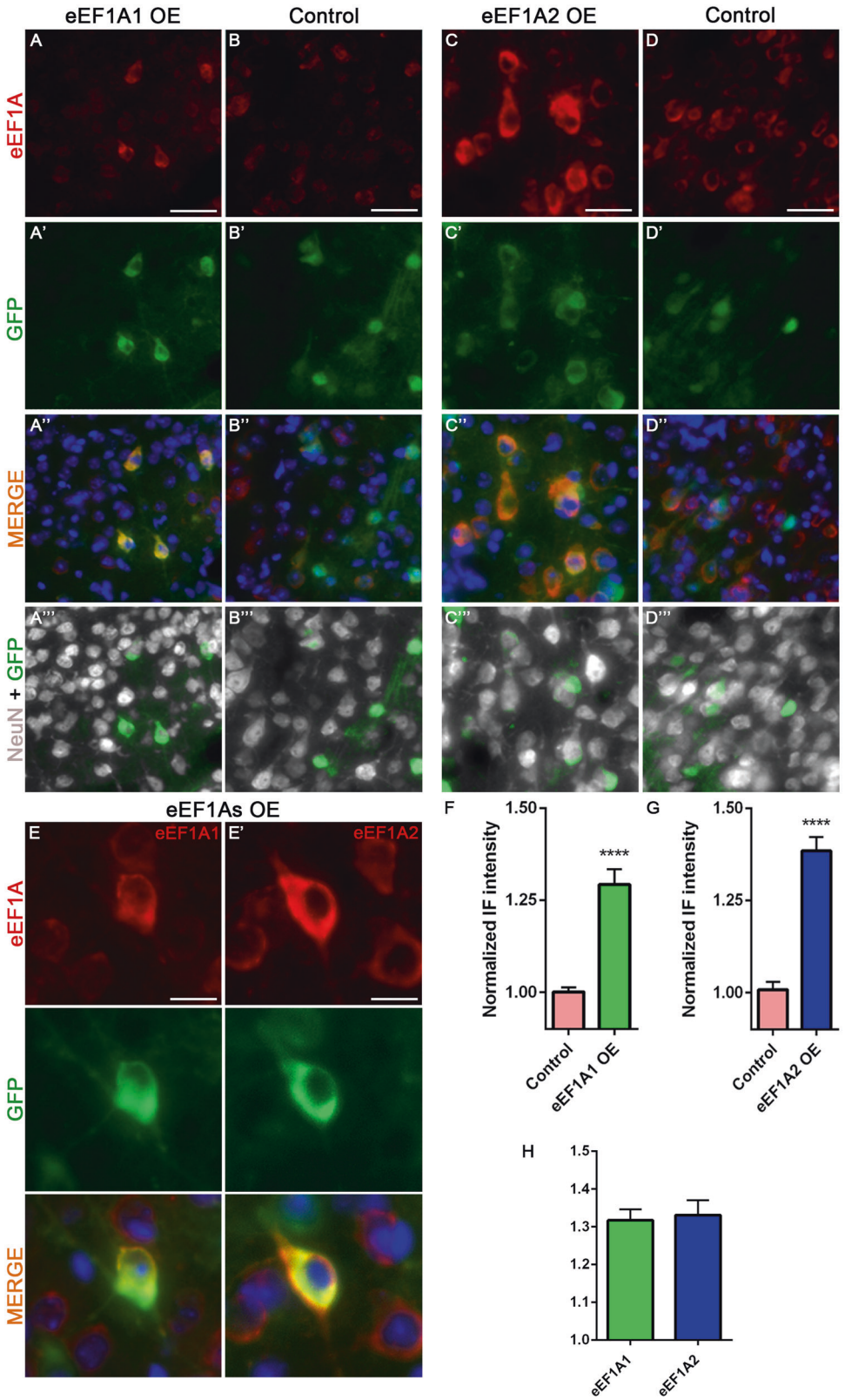

Fig. 1 Infection by AAV-eEF1A1 or AAV-eEF1A2 increases the level of eEF1A1 and eEF1A2 proteins, respectively, in CST neurons. Representative images of eEF1A1, GFP (viruses), and NeuN staining at the layer V of the right sensorimotor cortex of injured eEF1A1-overexpressing (OE) mice (**A**–**A**‴); and injured control mice (AAV-GFP injection) (**B**–**B**‴). Representative images of eEF1A2, GFP (viruses), and NeuN staining at the layer V of the right sensorimotor cortex of injured eEF1A2-OE mice (**C**–**C**‴); and injured control mice (AAV-GFP injection) (**D**–**D**‴). **E**, **E**′ Detailed images of eEF1A1 (**E**), eEF1A2 (**E**′) and GFP (viruses) staining in CST neurons of injured eEF1As OE mice. **F** Quantification of eEF1A1 immunoreactivity in eEF1A1 OE and control mice. **G** Quantification of eEF1A2 immunoreactivity in eEF1A2 OE and control mice. **H** Quantification of both eEF1A1 and eEF1A2 immunoreactivity in eEF1As OE mice. Scale bars: 50 μm (**A**–**D**‴), 25 μm (**E**–**E**′). Control, 12 mice; eEF1A1, 10 mice; eEF1A2, 10 mice; eEF1As OE 8 mice. 20 cells quantified per mouse. Stats: Mann–Whitney *U* test. Bars show mean ± SEM. ****$p < 0.0001$. Mann–Whitney *U* test revealed no significant differences between eEF1A1 and eEF1A2 intensities in eEF1As OE animals.

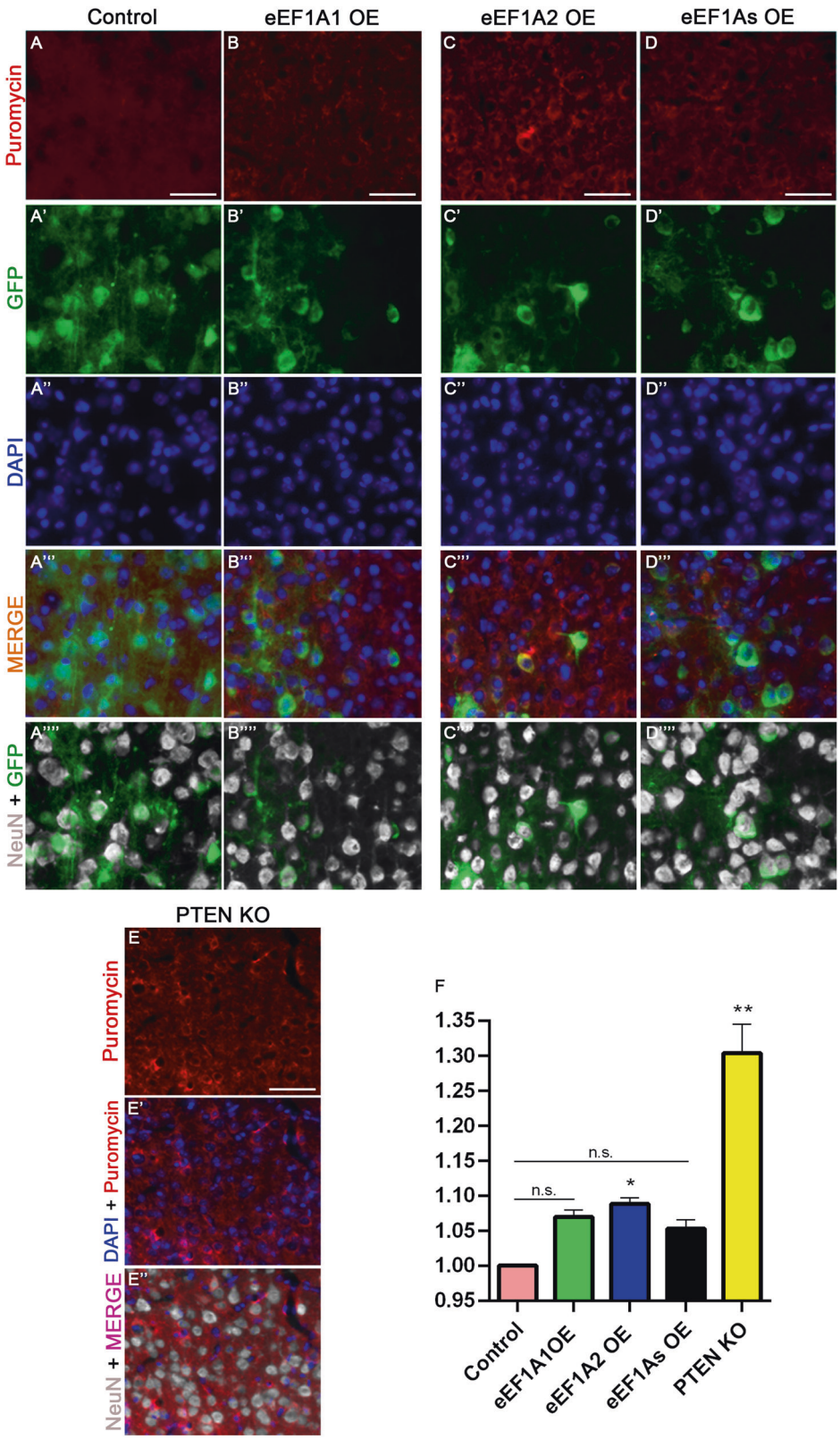

Fig. 2 Only eEF1A2 OE significantly increases protein synthesis. Representative images of puromycin, GFP (viruses), and NeuN staining at the layer V of the right sensorimotor cortex of injured control mice (AAV-GFP injection) (**A**–**A**‴); injured eEF1A1-overexpressing (OE) mice (**B**–**B**‴); injured eEF1A2-OE mice (**C**–**C**‴); injured eEF1As-OE mice (**D**–**D**‴); and injured PTEN cKO mice serving as a positive control (**E**–**E**″). **F** Quantification of puromycin immunoreactivity. Scale bars: 50 μm. 4 mice per each genetic condition; 50 cells quantified per mouse. Stats: One-way ANOVA with Kruskal–Wallis Test. Bars show mean ± SEM. *$p = 0.0239$, **$p = 0.0011$.

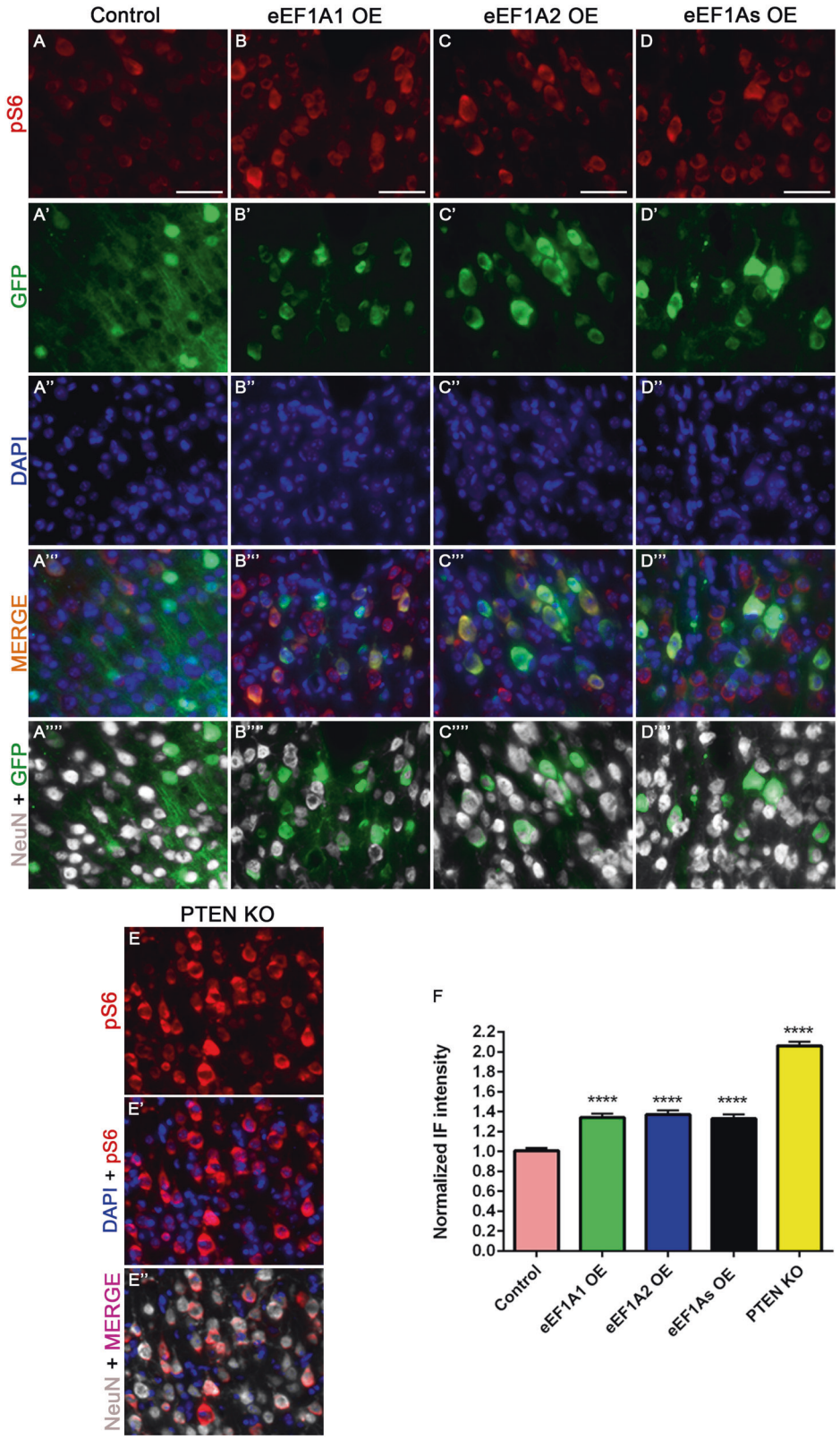

Fig. 3 Overexpression of eEF1A proteins activates mTOR signaling. Representative images of pS6, GFP (viruses), and NeuN staining at the layer V of the right sensorimotor cortex of injured control mice (AAV-GFP injection) (**A**–**A**‴); injured eEF1A1-overexpressing (OE) mice (**B**–**B**‴); injured eEF1A2-OE mice (**C**–**C**‴); injured eEF1As-OE mice (**D**–**D**‴); and injured PTEN cKO mice serving as a positive control (**E**–**E**″). **F** Quantification of pS6 immunoreactivity. Scale bars: 50 μm. Control, 12 mice; eEF1A1, 10 mice; eEF1A2, 10 mice; eEF1As, 8 mice; PTEN cKO, 4 mice; 20 cells quantified per mouse. Stats: One-way ANOVA with Kruskal–Wallis Test. Bars show mean ± SEM. ****$p < 0.0001$.

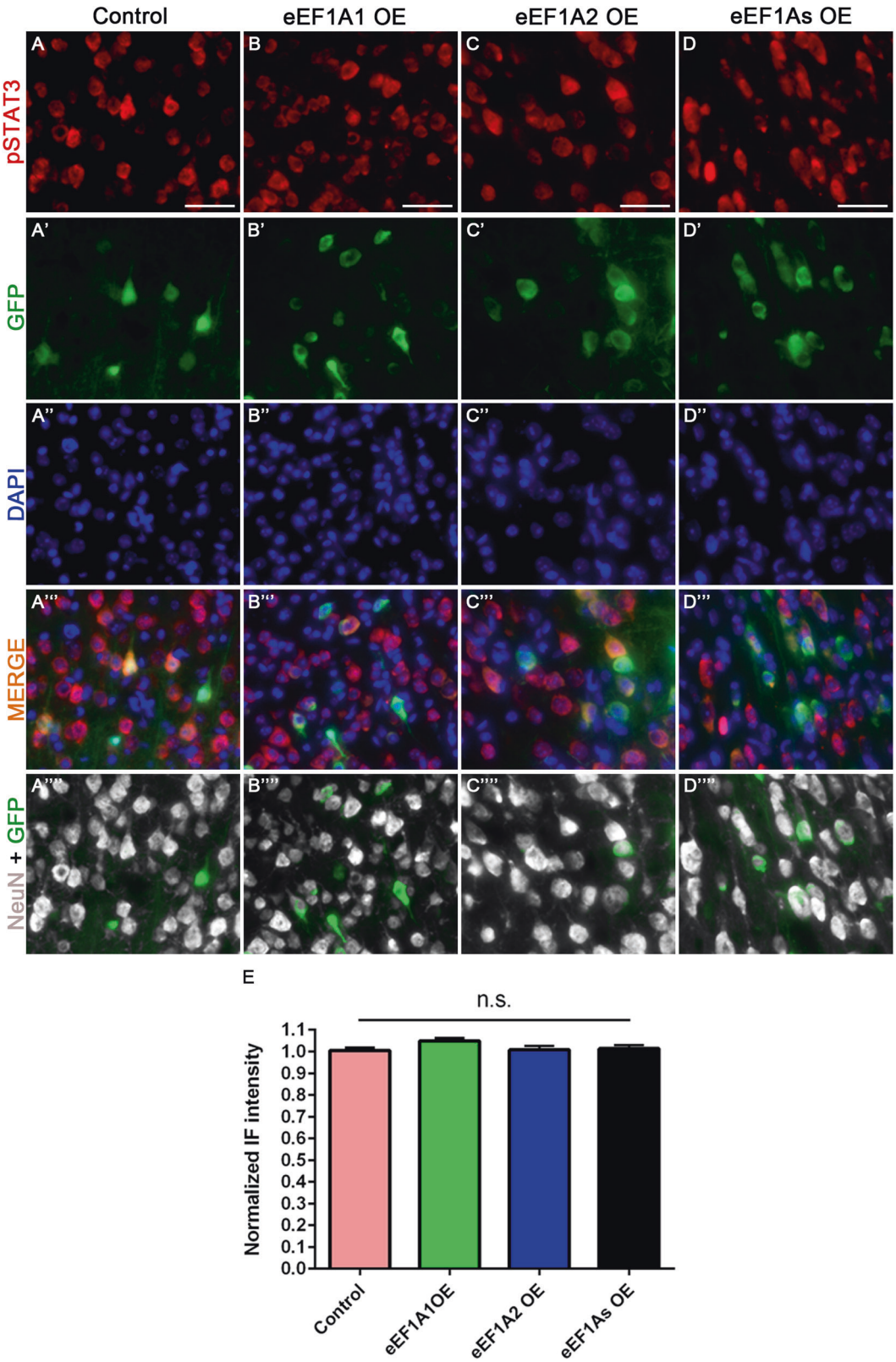

Fig. 4 Overexpression of eEF1A proteins does not activate STAT3 signaling. Representative images of pSTAT3, GFP (viruses), and NeuN staining at the layer V of the right sensorimotor cortex of injured control mice (AAV-GFP injection) (**A**–**A**''''); injured eEF1A1-OE mice (**B**–**B**''''); injured eEF1A2-OE mice (**C**–**C**''''); and injured eEF1As-OE mice (**D**–**D**''''). **E** Quantification of pSTAT3 immunoreactivity. Scale bars: 50 µm. Control, 12 mice; eEF1A1, 10 mice; eEF1A2, 10 mice; eEF1As, 8 mice; PTEN cKO, 4 mice per genetic condition; 20 cells quantified per mouse. Stats: One-way ANOVA with Kruskal–Wallis Test revealed no significant differences. Bars show mean ± SEM.

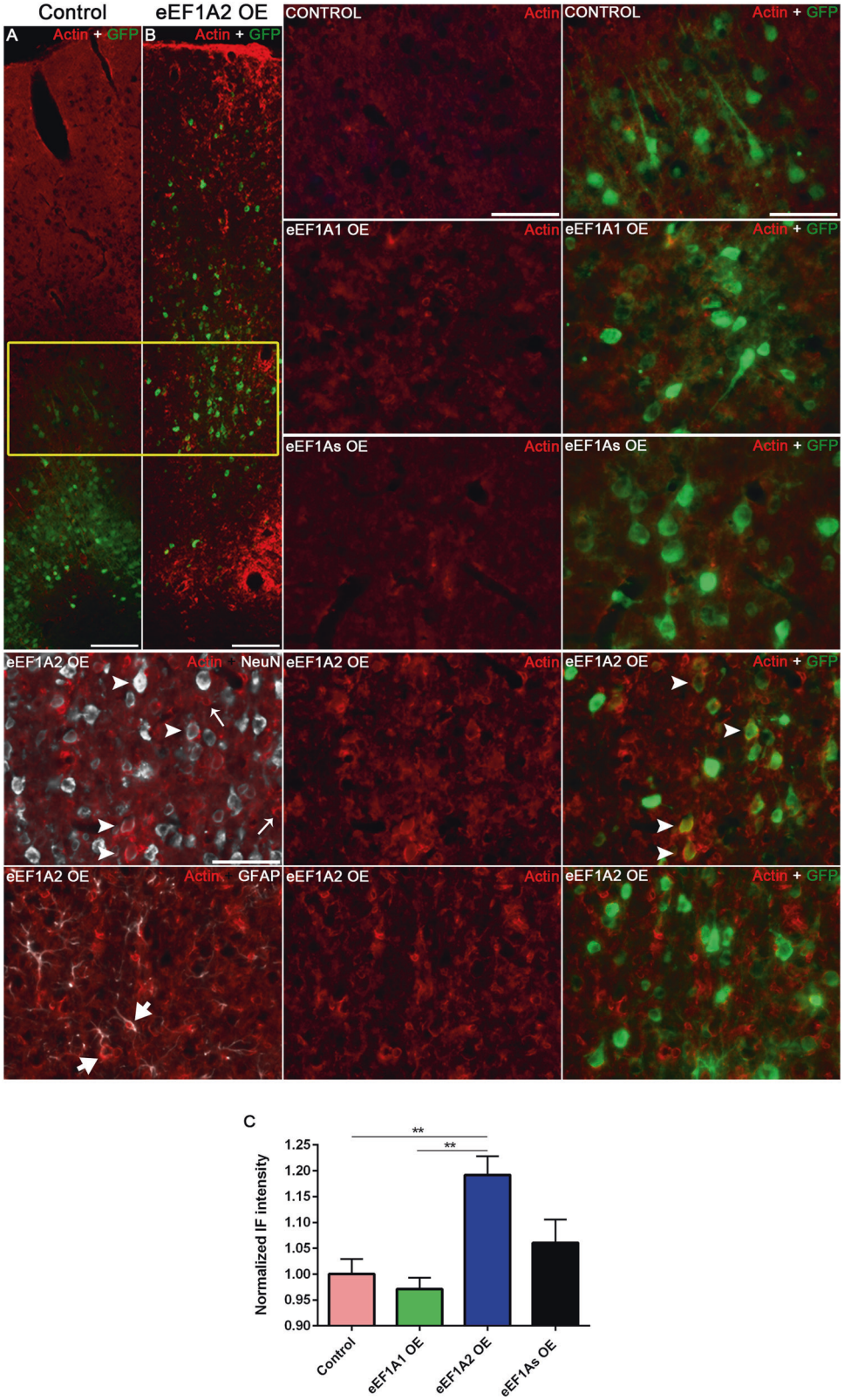

Fig. 5 Only eEF1A2 OE mice display actin rearrangement. Left panels: Representative 10× images of β-actin and GFP (viruses) staining at the right sensorimotor cortex of in control (**A**) and eEF1A2 OE (**B**) mice. Right and bottom panels: Detail from the cortical layer V (yellow box) at 20× magnification. Please note the bundled pattern of β-actin staining defining the cellular shape in $NeuN^+$ cells (arrowheads), $GFP^-/GFAP^+$ cells (thick arrows), and $GFP^-/GFAP^-/NeuN^-$ cells (thin arrows). Scale bars = 50 µm. **C** Quantification of β-actin immunoreactivity in cortical layer V. 3 mice per genetic condition. Stats: Ordinary one-way ANOVA. Bars show mean ± SEM. $^{**}p = 0.0054$, Control vs eEF1A2 OE; $^{**}p = 0.0018$, eEF1A1 OE vs eEF1A2 OE.

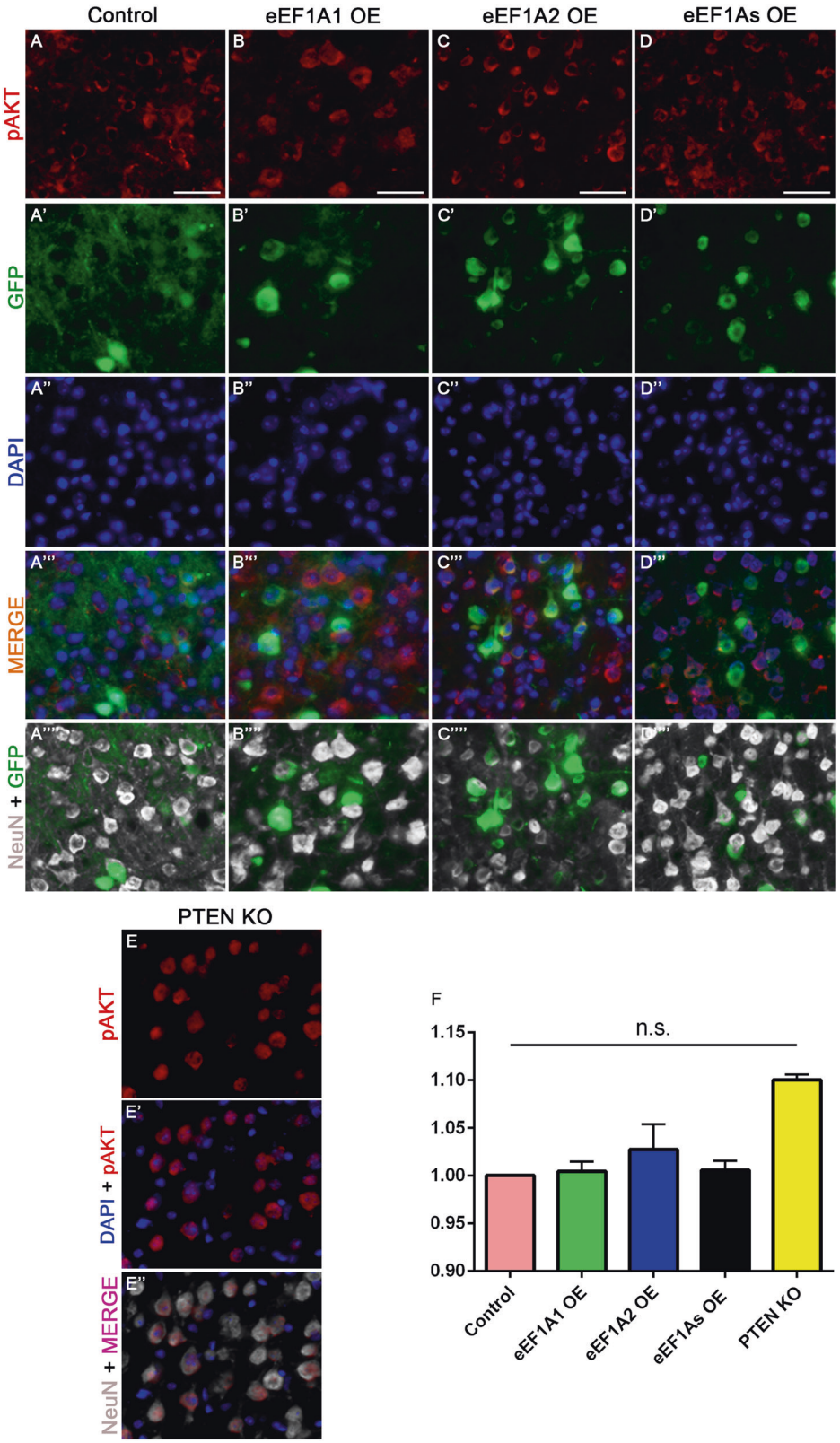

Fig. 6 Overexpression of eEF1A proteins does not increase pAKT phosphorylation. Representative images of pAKT, GFP (viruses), and NeuN staining at the layer V of the right sensorimotor cortex of injured control mice (AAV-GFP injection) (**A**–**A**‴); injured eEF1A1-overexpressing (OE) mice (**B**–**B**‴); injured eEF1A2-OE mice (**C**–**C**‴); injured eEF1As-OE mice (**D**–**D**‴); and injured PTEN cKO mice (**E**–**E**″). **F** Quantification of pAKT immunoreactivity. Scale bars: 50 μm. 4 mice per each genetic condition; 50 cells quantified per mouse. Stats: One-way ANOVA with Kruskal–Wallis Test. Bars show mean ± SEM.

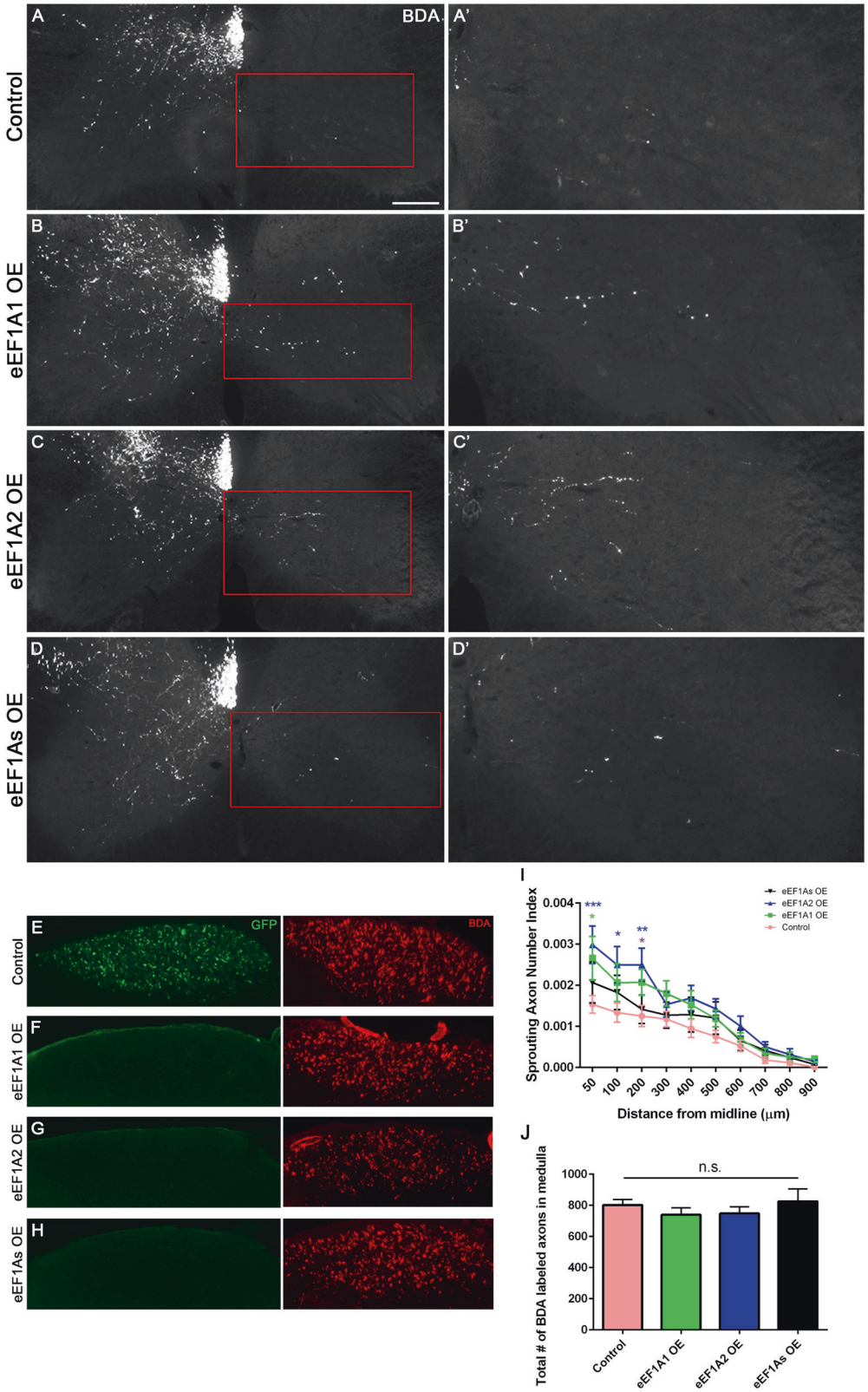

following a unilateral pyramidotomy injury. This represents the first proof-of-concept demonstration that forced expression of a core component of the protein translation machinery can exert a beneficial effect on axonal repair after CNS injury in vivo. In the case of eEF1A2, this could occur by a combination of enhancing protein synthesis, activating the mTOR pathway, and promoting actin remodeling. Here we discuss the implications and possible mechanisms underlying this eEF1A-mediated enhancement of CST axon sprouting.

First, it is important to note that our study focused on the sufficiency of overexpressing eEF1As to enhance sprouting with gain-of-function experiments rather than their necessity with loss-

Fig. 7 eEF1A2 OE mice exhibit increased compensatory CST axon sprouting more than eEF1A1 OE mice. Representative images of BDA tracing at the level of cervical spinal cord in control (**A**, **A'**), eEF1A1 OE (**B**, **B'**), eEF1A2 OE (**C**, **C'**), and eEF1As OE (**D**, **D'**) mice; scale bar = 300 µm. Right panel shows individual sprouting axons in the grey matter of the denervated half of spinal cord. **E**–**H** Representative images of GFP and BDA axonal labeling at the level of medullas. **I** Quantification of eEF1A1 OE, eEF1A2 OE, and eEF1As OE sprouting. Sprouting index indicates the ratio of the average number of axons counted at each distance past midline relative to the number of fibers labeled in the medulla. Compared to control, two-way RM ANOVA multiple comparisons with Tukey's correction revealed elevated sprouting for eEF1A1 OE: at 50 µm, $p = 0.0106$. Elevated sprouting for eEF1A2 OE compared to controls was observed at 50 µm, $p = 0.0006$; at 100 µm, $p = 0.0101$; and at 200 µm, $p = 0.0044$; compared to eEF1As OE mice, sprouting in eEF1A2 OE was higher at 200 µm, $p = 0.0403$. **J** Quantification of BDA-labeled axons at medullas. One-way ANOVA revealed no significant differences. Bars show mean ± SEM. Control mice: $n = 12$; eEF1A1 OE mice: $n = 10$; eEF1A2 OE mice: $n = 9$; eEF1As OE mice: $n = 8$; and PTEN cKO mice: $n = 4$.

of-function experiments. While addressing the necessity is generally important when functionally interrogating signaling pathways [31], it may not be a surprise if deleting a core component of the translational machinery proves to disrupt axonal repair along with other biological processes. Meanwhile, gain-of-function experiments such as those on c-Myc and an engineered form of KLF7 are valuable in revealing new molecular targets to enhance axonal repair after CNS injury [32, 33]. Here, our gain-of-function experiments on eEF1As provided evidence that overexpressing a core component of the translational machinery can promote axonal repair in the injured CNS. It is also of note that the levels of eEF1A1/2 overexpression are modest (or moderate at best), yet there is clear biological effect on axon sprouting especially in the case of eEF1A2. A priori it would be difficult to predict the optimal levels of overexpression for promoting axonal repair. Indeed, it is theoretically possible that a relatively low level of eEF1A overexpression is more conducive to axonal repair (as we did observe enhanced sprouting in the current study) while a high level may elicit pleiotropic effects. The optimal overexpression level for axonal repair remains to be established in future studies.

The in vivo puromycin incorporation assay showed that overexpressing eEF1A2 significantly increased protein synthesis in CST neurons, whereas overexpressing eEF1A1 or both eEF1As exhibited a trend for increased translation that did not reach statistical significance. While eEF1A2 OE increased translation only modestly at ~9%, it is conceivable that a modest increase in *global* protein synthesis can have a widespread and profound effect on cellular metabolisms. Even PTEN deletion, which serves as a benchmark for enhancing CST repair by increasing protein synthesis, only increased translation by ~30% in this assay. Meanwhile, there are very few reports in the literature applying the same puromycin-based SUnSET assay in vivo to compare our data to [25]. Interesting, eEF1A2 has been shown to regulate IRES-mediated translation of utrophin A gene [34], raising the possibility that eEF1A2 selectively impacts the translation of certain mRNA species in addition to its role in global protein synthesis. Recent work from Mendoza and colleagues [12] showed that eEF1A2 can stimulate protein translation in vitro, which agrees with our in vivo results in the neuronal soma. A less clear result with eEF1A1 overexpression on translation may reflect the well-documented but incompletely understood developmental switch from eEF1A1 to eEF1A2 in neurons and their different biochemical properties [4, 35–38]. Indeed, eEF1A2 deficiency in the postnatal stage leads to early neurodegeneration, muscle wasting, and subsequent animal death [39]. Biochemically, eEF1A1 and eEF1A2 differ in their affinity for GDP/GTP [40, 41] but also in their ability to interact with Ca^{2+}-calmodulin, which binds to eEF1A1 and displaces the tRNA [37]. Given that neurons are exposed to rapid changes in [Ca^{2+}], increases in Ca^{2+} could activate Ca^{2+}-calmodulin, which could then bind to eEF1A1 and impede its interaction with tRNA, thus reducing protein synthesis.

From cancer studies, it was established that eEF1A proteins can promote cell growth and proliferation by serving as an upstream activator of PI3K/AKT/mTOR [13, 42] and/or PI3K/AKT/STAT3 [14, 15] pathways. In partial agreement with those in vitro studies, our results showed that in an in vivo model of CNS injury, the overexpression of eEF1A proteins elevated mTOR activity, whereas co-overexpressing both proteins had no synergistic effect. However, the overexpression of neither eEF1A protein promoted activation of the STAT3 pathway. Several in vitro studies have shown the ability of eEF1A proteins to either enhance or attenuate the activity of various kinases such as AKT and PKR by direct interaction [16, 41, 43–45], although the underlying mechanism remains to be elucidated. Thus, it is possible that the overexpression of eEF1A proteins in CST neurons enhances the interactions between these elongation factors and such kinases along the mTOR pathway. Future studies will be needed to decipher the exact mechanism of action for eEF1A proteins in neuronal signaling.

The non-canonical role of eEF1A proteins related to actin dynamics has been most studied in the literature, mainly in yeast [16, 17, 20, 46, 47]. Importantly, in vitro studies confirmed that mammalian eEF1A proteins maintain the ability to interact with actin [12, 37, 48]. Moreover, a recent study has shown that the knockdown of eEF1A2 negatively impacted on neurite growth [20]. Here, we observed apparent bundling of beta actin in vivo in eEF1A2 OE mice, in contrast to control and eEF1A1 OE mice. These differences can be explained by a previous in vitro study reporting that mammalian eEF1A proteins differ in their capacity to interact with and modulate actin cytoskeleton [37]. Moreover, our results showed that additionally co-overexpressing eEF1A1 may attenuate the actin rearrangement seen in eEF1A2 OE mice. It is known that eEF1A1 and eEF1A2 can interact with one another and co-localize in the cytoplasm [49], so this result could suggest that eEF1A1 interacts with eEF1A2, thereby interfering with its interaction with actin. However, futures studies will be necessary to interrogate this interaction in CST neurons.

AKT kinase is a common upstream signaling molecule shared by actin rearrangement and mTOR pathways [16, 50–52]. We speculated that the eEF1A2-mediated elevation of both mTOR activity and actin bundling would be associated with a higher level of phosphorylated AKT. However, we did not detect elevated levels of pAKT following eEF1A1 or eEF1A2 OE. Recently, Huang and colleagues [51] reported that despite the important role of AKT in PTEN deletion-induced retinal axon regeneration, AKT activation is only marginal even in PTEN cKO mice, due to a mTORC1/S6K1-mediated feedback inhibition. This agrees with our results and can explain that only PTEN cKO mice exhibited a slight increase in pAKT. Based on the pAKT results, we cannot conclude whether the activity of actin bundling seen in eEF1A2 OE mice is primarily mediated by direct interaction between eEF1A2 and actin, or indirectly through AKT signaling. Further studies are needed to decipher the precise interaction between eEF1A proteins and the different kinases underlying cell growth and cytoskeleton dynamics.

Whereas eEF1A1 OE mice showed a modest enhancement of CST sprouting, eEF1A2 OE led to a clearer enhancement of CST sprouting, approaching that seen in PTEN cKO mice. The pattern of effects on protein synthesis, mTOR signaling and actin dynamics may support the hypothesis that eEF1A2 promotes sprouting through a combination of these three aspects rather than mTOR signaling alone, where the effects of overexpressing

eEF1A1 or eEF1A2 are indistinguishable. Accordingly, results from eEF1A2 OE mice indicate a higher rate in actin bundling, which may facilitate the generation of collaterals to innervate the denervated side [53], akin to what has been described on dendritic spines [12]. In this regard, our study echoes strongly with the study by Mendoza and colleagues [12] in that eEF1A2 serves as a link to coordinate protein translation and actin dynamics in regulating neuronal functions. Whereas Mendoza studied this link in the context of structural plasticity in dendritic spines in cultured neurons, our data implicate this link in the context of axonal regeneration after CNS injury in vivo. Intriguingly, additionally overexpressing eEF1A1 reduced the elevated level of sprouting seen in eEF1A2 OE mice, which was accompanied by an apparent reduction in protein synthesis and actin rearrangement. Furthermore, our results unexpectedly showed that the enhancement in CST sprouting is likely driven from the neuronal somas rather than axons [7, 53–55] since neither eEF1A1::GFP nor eEF1A2::GFP fusion proteins are localized to the level of medulla in CST axons. Although the GFP tag and the lack of endogenous untranslated regions (UTRs) in our eEF1A constructs could in principle affect function thereby representing potential caveats, we and others [56] did not find abnormal functions or subcellular localizations of the eEF1A proteins overexpressed through viral constructs.

CONCLUSION

Together, our findings indicate that neuronal eEF1A2 promotes axon sprouting after CNS injury and suggest that it does so by acting as a hub connecting mTOR signaling, protein synthesis and actin cytoskeleton. The level of eEF1A2-mediated enhancement in CST sprouting approached but did not exceed PTEN deletion. Our study provides the first demonstration that manipulating a core component of the translational machinery can enhance axonal sprouting in the mammalian CNS, supporting the hypothesis that protein synthesis is important for axonal repair. Unexpectedly, eEF1A2 appears to carry out these functions from the neuronal somas and not at the axons, while eEF1A1 exerts a somewhat antagonistic role that remains to be fully understood. Future studies will be required to determine whether eEF1A2 overexpression can also promote axon regeneration from injured CST neurons following spinal cord injury.

MATERIALS AND METHODS

Mice

All mouse husbandry and experimental procedures were approved by the Institutional Animal Care and Use Committee at the University of California San Diego. Forty wild-type C57BL/6 male and female mice (6 weeks old) in an ~1:1 ratio was randomly divided for each condition as follows: 12 mice for the control group, 10 mice for the eEF1A1 group, 10 mice for the eEF1A2 group, and 8 mice for the eEF1As group. In any one surgical session, mice for the different conditions (including controls) were represented in order to minimize any effect of surgical variations. In some procedures, these mice were compared against PTEN conditional knockout (cKO) mice in the same genetic background.

Viral production

pCMV6-eEF1A1 (#MG207381) and pCMV6-eEF1A2 (#MG207396) mouse ORF clones (GFP tagged) were obtained from OriGene (USA) and subcloned into AAV2 (shortened as AAV) vectors at the Boston Children's Hospital Viral Core, from where AAV-Cre and AAV-GFP were also acquired (Fig. S1B). Viral titers were confirmed using qPCR to be 1.6×10^{12} TU/ml (eEF1A1-overexpressing AAV vector; eEF1A1 OE), 1.2×10^{12} TU/ml (eEF1A2-overexpressing AAV vector; eEF1A2 OE), and 0.5×10^{12} TU/ml (AAV-Cre and AAV-GFP). The viral titer of eEF1A1 OE was diluted to the one of eEF1A2 OE (1.2×10^{12} TU/ml) in order to have the same viral titer in the individual treatments. Likewise, this viral titer (1.2×10^{12} TU/ml) was maintained during the combination treatment for each construct (eEF1A1 OE + eEF1A2 OE).

Surgical procedures

Virus was delivered following general anesthesia by intraperitoneal injection of ketamine and xylazine dosed at 80–100 mg/kg and 10 mg/kg, respectively. Briefly, a total of 1.2 µL of each vector separately (eEF1A1 OE and eEF1A2 OE), or co-injections of both vectors (eEF1As OE), or AAV-GFP as control were injected at three different sites (0.4 µL per site) into the right sensorimotor cortex of 6-week-old wild-type mice [57]. Injection coordinates relative to bregma were as follows: 1.2 mm lateral, 0.5 mm anterior, 1.2 mm lateral, 0.5 mm posterior, 2.2 mm lateral, 0.0 mm anterior. For each injection site, the needle was lowered to a depth of 0.7 mm. $PTEN^{fl/fl}$ mice underwent the same procedures with AAV-Cre to generate PTEN cKO mice, or with AAV-GFP as controls.

Unilateral pyramidotomy and biotinylated dextran amine (BDA) tracer injection were performed as described previously [57–59]. Following general anesthesia, 8-week-old mice underwent pyramidotomy by cutting the entire left pyramidal tract just caudal to the foramen magnum. Cortical injection of BDA (10%, Invitrogen) was performed 2 weeks prior to sacrifice for all studies using the same procedures as for AAV injection. Surgeons performing the surgeries were blinded to conditions. Mice were sacrificed at 12 weeks of age (Fig. S1A).

In vivo puromycin administration and tissue processing

A group of mice were injected intraperitoneally with 225 mg/kg puromycin (Thomas Scientific, C791P84) suspended in water 25 min before being sacrificed, as previously described [25]. For all experiments, mice were sacrificed by an overdose of Fatal Plus (pentobarbital sodium, intraperitoneal injection of 150 mg/kg mouse), and then transcardially perfused with an ice-cold solution of 4% paraformaldehyde (PFA). Finally, brains and spinal cords were dissected out, and the tissues were post-fixed overnight at 4 °C in the same fixative solution.

Tissue processing was performed as described previously [57, 58]. Briefly, tissues were incubated in 30% sucrose for cryo-protection. Brain, medulla, and C5-C7 cervical spinal cord were embedded in OCT compound and frozen. Tissues were transversely sectioned with a cryostat at a thickness of 20 µm. For tissues containing BDA labeled axons, cervical spinal cord and medulla sections were incubated in Vectastain ABC solution (Vector Laboratories) overnight at 4 °C. BDA was detected with TSA Plus Fluorescein System (1:200, PerkinElmer). For immunohistochemistry, sections were first washed with 0.2% triton-PBS and then blocked and permeabilized (0.4% triton, 5% sera matching the species of the secondary antibodies, 1× PBS) for 1 h at room temperature. Incubation in the primary antibody solution (see concentrations below) was carried out at 4 °C overnight. Sections were washed, followed by secondary antibody staining for 2 h at room temperature (antibody solutions at 1:500). Next, sections were washed again, incubated with DAPI for 10 min, and mounted with Fluoromount-G (Southern Biotech).

The following antibodies were used: rabbit anti-eEF1A1 (1:100, abcam), rabbit anti-eEF1A2 (1:100, Sigma-Aldrich), monoclonal mouse anti-Puromycin, clone 12D10 (1:100, EMD Millipore), guinea pig anti-NeuN (1:200, Sigma-Aldrich), rabbit anti-pS6 (Ser235/236) (1:200, Cell Signaling Technology), rabbit anti-pSTAT3 (Tyr705) (1:200, Cell Signaling Technology), rabbit anti-pAKT1 (Ser473) (1:100, Cell Signaling Technology), rat anti-GFAP (1:500, Thermo Fisher), and rabbit anti-beta Actin (1:100, abcam). For sprouting studies, selected transverse sections of cervical spinal cord (C7) were immunostained for PKCγ (1:100, Santa Cruz Biotechnology) to examine the completeness of the lesion for each mouse [59]. Mice with incomplete lesion were excluded from the study.

For pSTAT3 and beta Actin staining that required antigen retrieval, the protocol was performed as described previously [60]. Briefly, brain sections were pre-treated with 1% NaOH, followed by washes with PBS, then incubated with 0.3% glycine, rinsed with PBS, and next treated with 0.03% sodium dodecyl sulfate (SDS). After three additional washes, sections were blocked in 0.2% Triton X-100 in PBS for 1 h at room temperature, incubated with anti-pSTAT3 or anti-beta actin antibodies for overnight at RT, and then following the regular protocol.

For puromycin staining, the Mouse on Mouse (MOM) Detection Kit (Vector Labs, BMK-2202) was used for blocking and staining procedures as previously described [25], with buffers prepared as described in standard protocol supplied with the kit.

Image acquisition

Stained tissue sections were photographed using an upright epifluorescence microscope (Zeiss Axio Imager M1). For coronal brain sections, one section per injection site (three sections total) showing GFP signal along

the layer V of the cerebral cortex were photographed for each animal. Five transverse sections of the medullary pyramids were randomly photographed. For cervical spinal cord sections, 10 transverse sections per animal between C5-C7 levels were randomly photographed. Photomicrographs were taken at 10× (brain, medulla, and cervical sections), and 20× or 100× (brain sections) magnification without changing the amplifier gain or the offset to avoid the introduction of experimental variability. Stacks of microphotographs were processed with Fiji (ImageJ) software.

Following quantifications, contrast and brightness were minimally adjusted in figures, uniformly across panels for each experiment, with Adobe Photoshop CS4 (Adobe Systems).

Immunofluorescence quantifications

To quantify the intensity of each immunofluorescence (IF) signal in layer V CST neurons, mean fluorescent intensity (mean grey value) from GFP^+ CST neurons was determined using ImageJ. The actin quantification was performed in an GFP^+ area within layer V and not cell by cell. All values underwent internal normalization to GFP^- CST neurons or GFP^- area, respectively, and then they were normalized against control values. The experimenter was blinded during quantifications.

We carried out an estimation of viral infection efficiency by selecting an area within layer V to quantify the number of GFP+/NeuN+ neurons. Then, this value was normalized against the total number of NeuN+ neurons. In this way, we obtained an estimated infection efficiency of 40%.

For the quantification of BDA-labeled axon numbers, we adapted a semiautomatic quantification method previously used [61]. Positive profiles of the medulla were quantified by using the "analyze particle" function of ImageJ, and the average number of BDA positive axons per section was calculated for each animal: 802.2 ± 35.83 (control); 739.9 ± 44.16 (eEF1A1 OE mice); 748.1 ± 43.35 (eEF1A2 OE mice); 825.3 ± 80.97 (eEF1As OE mice); and 652.9 ± 72.12 (PTEN cKO mice) (Fig. 7J, S2E). Both the initial observation of the stained sections and later quantification of axon numbers were conducted by experimenters blinded to conditions.

Sprouting Axon Number Index was quantified similarly as described [57, 58]. Briefly, the number of axons crossing pre-defined lines at various distances from the midline on the denervated gray matter was manually counted in 10 randomly chosen C5-C7 transverse sections per animal by a blinded observer. Counts were averaged for each animal and normalized against the total labeled CST axon count in the medulla [59] to obtain the sprouting index, which was plotted as a function of distance from the midline.

Statistical analyses

Sample size was calculated using the application available in http://www.biomath.info/power/ttest.htm, based upon $\alpha = 0.05$ and power of $\beta = 0.8$. Statistical analysis was carried out using Prism 6 (GraphPad software, La Jolla, CA). Data were presented as mean ± S.E.M. Normality of the data was determined by two different tests depending on the n numbers: the D'Agostino-Pearson omnibus test when n numbers were equal or higher than 10, and the Kolmogorov-Smirnov test when *n* numbers were below 10. The immunohistochemistry data with multiple comparisons were analyzed by either one-way ANOVA or Kruskal–Wallis test where appropriate, and post-hoc Dunn's multiple comparisons test. The results of control vs. eEF1A overexpression groups were analyzed by Mann–Whitney *U* test. Sprouting index data were analyzed via two-way repeated measures ANOVA with Tukey post-hoc test. Correlations were assessed with the Spearman correlation coefficient test or the Pearson correlation coefficient test where appropriate. The significance level was set at 0.05. In the figures, significance values were represented by different number of asterisks: *$p < 0.05$; **$p < 0.01$; ***$p < 0.001$; ****$p < 0.0001$.

DATA AVAILABILITY

The datasets generated and/or analysed during the current study are available from the corresponding author on reasonable request.

REFERENCES

1. He Z, Jin Y. Intrinsic control of axon regeneration. Neuron. 2016;90:437–51.
2. Andersen GR, Nissen P, Nyborg J. Elongation factors in protein biosynthesis. Trends Biochem Sci. 2003;28:434–41.
3. Dever TE, Dinman JD, Green R. Translation elongation and recoding in eukaryotes. Cold Spring Harb Perspect Biol. 2018;10:a032649.
4. Lee S, Francoeur AM, Liu S, Wang E. Tissue-specific expression in mammalian brain, heart, and muscle of S1, a member of the elongation factor-1α gene family. J Biol Chem. 1992;267:24064–8.
5. Knudsen SM, Frydenberg J, Clark BFC, Leffers H. Tissue-dependent variation in the expression of elongation factor-1 alpha isoforms: isolation and characterisation of a cDNA encoding a novel variant of human elongation-factor 1 alpha. Eur J Biochem. 1993;215:549–54.
6. Newbery HJ, Loh DH, O'Donoghue JE, Tomlinson VAL, Chau YY, Boyd JA, et al. Translation elongation factor eEF1A2 is essential for post-weaning survival in mice. J Biol Chem. 2007;282:28951–9.
7. Zheng JQ, Kelly TK, Chang B, Ryazantsev S, Rajasekaran AK, Martin KC, et al. A functional role for intra-axonal protein synthesis during axonal regeneration from adult sensory neurons. J Neurosci. 2001;21:9291–303.
8. Liu K, Lu Y, Lee JK, Samara R, Willenberg R, Sears-Kraxberger I, et al. PTEN deletion enhances the regenerative ability of adult corticospinal neurons. Nat Neurosci. 2010;13:1075–81.
9. Park KK, Liu K, Hu Y, Smith PD, Wang C, Cai B, et al. Promoting axon regeneration in the adult CNS by modulation of the PTEN/mTOR pathway. Science. 2008;322:963–6.
10. Kapur M, Monaghan CE, Ackerman SL. Regulation of mRNA Translation in. Neurons-A Matter Life Death Neuron. 2017;96:616–37.
11. Yang L, Miao L, Liang F, Huang H, Teng X, Li S, et al. The mTORC1 effectors S6K1 and 4E-BP play different roles in CNS axon regeneration. Nat Commun. 2014;5:5416.
12. Mendoza MB, Gutierrez S, Ortiz R, Moreno DF, Dermit M, Dodel M, et al. The elongation factor eEF1A2 controls translation and actin dynamics in dendritic spines. Sci Signal. 2021;14:eabf5594.
13. Pellegrino R, Calvisi DF, Neumann O, Kolluru V, Wesely J, Chen X, et al. EEF1A2 inactivates p53 by way of PI3K/AKT/mTOR-dependent stabilization of MDM4 in hepatocellular carcinoma. Hepatology. 2014;59:1886–99.
14. Anand N, Murthy S, Amann G, Wernick M, Porter LA, Cukier IH, et al. Protein elongation factor EEF1A2 is a putative oncogene in ovarian cancer. Nat Genet. 2002;31:301–5.
15. Li Z, Qi CF, Shin DM, Zingone A, Newbery HJ, Kovalchuk AL, et al. Eef1a2 promotes cell growth, inhibits apoptosis and activates JAK/STAT and AKT signaling in mouse plasmacytomas. PLoS ONE. 2010;5:e10755.
16. Amiri A, Noei F, Jeganathan S, Kulkarni G, Pinke DE, Lee JM. eEF1A2 activates Akt and stimulates Akt-dependent actin remodeling, invasion and migration. Oncogene. 2007;26:3027–40.
17. Condeelis J. Elongation factor 1 alpha, translation and the cytoskeleton. Trends Biochem Sci. 1995;20:169–70.
18. Gross SR, Kinzy TG. Translation elongation factor 1A is essential for regulation of the actin cytoskeleton and cell morphology. Nat Struct Mol Biol. 2005;12:772–8.
19. Jeganathan S, Morrow A, Amiri A, Lee JM. Eukaryotic elongation factor 1A2 cooperates with phosphatidylinositol-4 kinase III beta to stimulate production of filopodia through increased phosphatidylinositol-4,5 bisphosphate generation. Mol Cell Biol. 2008;28:4549–61.
20. Murray JW, Edmonds BT, Liu G, Condeelis J. Bundling of actin filaments by elongation factor 1 alpha inhibits polymerization at filament ends. J Cell Biol. 1996;135:1309–21.
21. Rumpansuwon K, Prommahom A, Dharmasaroja P. eEF1A2 knockdown impairs neuronal proliferation and inhibits neurite outgrowth of differentiating neurons. Neuroreport. 2022;33:336–44.
22. Nawabi H, Belin S, Cartoni R, Williams PR, Wang C, Latremolière A, et al. Doublecortin-like kinases promote neuronal survival and induce growth cone reformation via distinct mechanisms. Neuron. 2015;88:704–19.
23. Ertürk A, Hellal F, Enes J, Bradke F. Disorganized microtubules underlie the formation of retraction bulbs and the failure of axonal regeneration. J Neurosci. 2007;27:9169–80.
24. Dent EW, Gupton SL, Gertler FB. The growth cone cytoskeleton in axon outgrowth and guidance. Cold Spring Harb Perspect Biol. 2011;3:1–39.
25. Koren SA, Hamm MJ, Meier SE, Weiss BE, Nation GK, Chishti EA, et al. Tau drives translational selectivity by interacting with ribosomal proteins. Acta Neuropathol. 2019;137:571–83.
26. Schmidt EK, Clavarino G, Ceppi M, Pierre P. SUnSET, a nonradioactive method to monitor protein synthesis. Nat Methods. 2009;6:275–7.
27. Jin D, Liu Y, Sun F, Wang X, Liu X, He Z. Restoration of skilled locomotion by sprouting corticospinal axons induced by co-deletion of PTEN and SOCS3. Nat Commun. 2015;6:8074.
28. Song MS, Salmena L, Pandolfi PP. The functions and regulation of the PTEN tumour suppressor. Nat Rev Mol Cell Biol. 2012;13:283–96.
29. Giustetto M, Hegde AN, Si K, Casadio A, Inokuchi K, Pei W, et al. Axonal transport of eukaryotic translation elongation factor 1alpha mRNA couples transcription in the nucleus to long-term facilitation at the synapse. Proc Natl Acad Sci USA. 2003;100:13680–5.
30. Cho SJ, Lee HS, Dutta S, Seog DH, Moon IS. Translation elongation factor-1A1 (eEF1A1) localizes to the spine by domain III. BMB Rep. 2012;45:227–32.

31. Saikia JM, Chavez-Martinez CL, Kim ND, Allibhoy S, Kim HJ, Simonyan L, et al. A critical role for DLK and LZK in axonal repair in the mammalian spinal cord. J Neurosci. 2022;42:3716–32.
32. Belin S, Nawabi H, Wang C, Tang S, Latremoliere A, Warren P, et al. Neuron. 2015;86:1000–14.
33. Blackmore MG, Wang Z, Lerch JK, Motti D, Zhang YP, Shields CB, et al. Proc Natl Acad Sci USA. 2012;109:7517–22.
34. Péladeau C, Adam N, Bronicki LM, Coriati A, Thabet M, Al-Rewashdy H, et al. Identification of therapeutics that target eEF1A2 and upregulate utrophin A translation in dystrophic muscles. Nat Commun. 2020;11:1990.
35. Khalyfa A, Bourbeau D, Chen E, Petroulakis E, Pan J, Xu S, et al. Characterization of elongation factor-1A (eEF1A-1) and eEF1A-2/S1 protein expression in normal and wasted mice. J Biol Chem. 2001;276:22915–22.
36. Abbott CM, Newbery HJ, Squires CE, Browsntein D, Griffiths LA, Soares DC. eEF1A2 and neuronal degeneration. Biochem Soc Trans. 2009;37:1293–7.
37. Novosylna O, Doyle A, Vlasenko D, Murphy M, Negrutskii B, El'Skaya A. Comparison of the ability of mammalian eEF1A1 and its oncogenic variant eEF1A2 to interact with actin and calmodulin. Biol Chem. 2017;398:113–24.
38. McLachlan F, Sires AM, Abbott CM. The role of translation elongation factor eEF1 subunits in neurodevelopmental disorders. Hum Mutat. 2019;40:131–41.
39. Chambers DM, Peters J, Abbott CM. The lethal mutation of the mouse wasted (wst) is a deletion that abolishes expression of a tissue-specific isoform of translation elongation factor 1alpha, encoded by the Eef1a2 gene. Proc Natl Acad Sci USA. 1998;95:4463–8.
40. Kahns S, Lund A, Kristensen P, Knudsen CR, Clark BFC, Cavallius J, et al. The elongation factor 1 A-2 isoform from rabbit: cloning of the cDNA and characterization of the protein. Nucleic Acids Res. 1998;26:1884–90.
41. Leclercq TM, Moretti PAB, Pitson SM. Guanine nucleotides regulate sphingosine kinase 1 activation by eukaryotic elongation factor 1A and provide a mechanism for eEF1A-associated oncogenesis. Oncogene. 2011;30:372–8.
42. Yang J, Tang J, Li J, Cen Y, Chen J, Dai G. Effect of activation of the Akt/mTOR signaling pathway by EEF1A2 on the biological behavior of osteosarcoma. Ann Transl Med. 2021;9:158–158.
43. Losada A, Muñoz-Alonso MJ, Martínez-Díez M, Gago F, Domínguez JM, Martínez-Leal JF, et al. Binding of eEF1A2 to the RNA-dependent protein kinase PKR modulates its activity and promotes tumour cell survival. Br J Cancer. 2018;119:1410–20.
44. Panasyuk G, Nemazanyy I, Filonenko V, Negrutskii B, El'skaya AV. A2 isoform of mammalian translation factor eEF1A displays increased tyrosine phosphorylation and ability to interact with different signalling molecules. Int J Biochem Cell Biol. 2008;40:63–71.
45. Lau J, Castelli LA, Lin ECK, Macaulay SL. Identification of elongation factor 1alpha as a potential associated binding partner for Akt2. Mol Cell Biochem. 2006;286:17–22.
46. Munshi R, Kandl KA, Carr-Schmid A, Whitacre JL, Adams AEM, Kinzy TG. Overexpression of translation elongation factor 1A affects the organization and function of the actin cytoskeleton in yeast. Genetics. 2001;157:1425–36.
47. Liu G, Grant WM, Persky D, Latham VM, Singer RH, Condeelis J. Interactions of elongation factor 1alpha with F-actin and beta-actin mRNA: implications for anchoring mRNA in cell protrusions. Mol Biol Cell. 2002;13:579–92.
48. Vlasenko DO, Novosylna OV, Negrutskii BS, El'skaya AV. Truncation of the A,A(*),A' helices segment impairs the actin bundling activity of mammalian eEF1A1. FEBS Lett. 2015;589:1187–93.
49. Migliaccio N, Ruggiero I, Martucci NM, Sanges C, Arbucci S, Tatè R, et al. New insights on the interaction between the isoforms 1 and 2 of human translation elongation factor 1A. Biochimie. 2015;118:1–7.
50. Endersby R, Baker SJ. PTEN signaling in brain: neuropathology and tumorigenesis. Oncogene. 2008;27:5416–30.
51. Huang H, Miao L, Yang L, Liang F, Wang Q, Zhuang P, et al. AKT-dependent and -independent pathways mediate PTEN deletion-induced CNS axon regeneration. Cell Death Dis. 2019;10:203.
52. Ijuin T. Phosphoinositide phosphatases in cancer cell dynamics-beyond PI3K and PTEN. Semin Cancer Biol. 2019;59:50–65.
53. Leite SC, Pinto-Costa R, Sousa MM. Actin dynamics in the growth cone: a key player in axon regeneration. Curr Opin Neurobiol. 2021;69:11–18.
54. Willis DE, Twiss JL. The evolving roles of axonally synthesized proteins in regeneration. Curr Opin Neurobiol. 2006;16:111–8.
55. Cheever TR, Ervasti JM. Actin isoforms in neuronal development and function. Int Rev Cell Mol Biol. 2013;301:157–213.
56. Duman M, Vaquié A, Nocera G, Heller M, Stumpe M, Siva Sankar D, et al. EEF1A1 deacetylation enables transcriptional activation of remyelination. Nat Commun. 2020;11:3420.
57. Geoffroy CG, Lorenzana AO, Kwan JP, Lin K, Ghassemi O, Ma A, et al. Effects of PTEN and Nogo codeletion on corticospinal axon sprouting and regeneration in mice. J Neurosci. 2015;35:6413–28.
58. Meves JM, Geoffroy CG, Kim ND, Kim JJ, Zheng B. Oligodendrocytic but not neuronal Nogo restricts corticospinal axon sprouting after CNS injury. Exp Neurol. 2018;309:32–43.
59. Lee JK, Geoffroy CG, Chan AF, Tolentino KE, Crawford MJ, Leal MA, et al. Assessing spinal axon regeneration and sprouting in Nogo-, MAG-, and OMgp-deficient mice. Neuron. 2010;66:663–70.
60. Chen M, Geoffroy CG, Meves JM, Narang A, Li Y, Nguyen MT, et al. Leucine zipper-bearing kinase is a critical regulator of astrocyte reactivity in the adult mammalian CNS. Cell Rep. 2018;22:3587–97.
61. Cornide-Petronio ME, Fernández-López B, Barreiro-Iglesias A, Rodicio MC. Traumatic injury induces changes in the expression of the serotonin 1A receptor in the spinal cord of lampreys. Neuropharmacology. 2014;77:369–78.

ACKNOWLEDGEMENTS

This work has been Supported by grants from NIH/NINDS (NS093055), VA (RX002483), Wings for Life and Craig H. Neilsen foundations to BZ. Viral preps were obtained from Boston Children's Hospital Viral Core (EY012196). The contents do not represent the views of the U.S. Department of Veterans Affairs or the United States Government.

AUTHOR CONTRIBUTIONS

DR-S and BZ designed and conceptualized the research framework, interpreted results of experiments, and drafted the manuscript; DR-S, JMS, HJK, KMT, and GQL performed experiments and genotyping; and DR-S analyzed data.

COMPETING INTERESTS

The authors declare no competing interests.

ADDITIONAL INFORMATION

Supplementary information The online version contains supplementary material available at https://doi.org/10.1038/s41420-022-01186-z.

Correspondence and requests for materials should be addressed to Binhai Zheng.

Reprints and permission information is available at http://www.nature.com/reprints

Publisher's note Springer Nature remains neutral with regard to jurisdictional claims in published maps and institutional affiliations.